

REAL-TIME INSTRUMENT FOR STRUCTURAL HEALTH MONITORING

B. W. Lee^{1*}, M. S. Seo¹, H. G. Oh¹, C. Y. Park²

¹ Fiberpro Inc, Daejeon, Korea, ² Aeronautical Technology Directorate, ADD, Daejeon, Korea

* Corresponding author (bwlee@fiberpro.com)

Keywords: *FBG sensor, PZT sensor, spectrum, interrogator, SHM*

1 Objective

The main advantages of fiber Bragg grating (FBG) sensors come from simple wiring harnesses, low electromagnetic interference susceptibility and high multiplexing capability. While FBGs are widely adopted for structural health monitoring (SHM) application with such unique merits, physical measurands should be transduced to strain in the optical fiber. In case that strain information is not much related to structural health, it is necessary to rely on other sensors such as piezoelectric transducer (PZT) sensors.

In case of unmanned aerial vehicles, an onboard SHM instrument is demanded to autonomously generate alarm signals depending on structural damage levels and record structural deformation data like a black box for in-depth analysis and management on ground basis. As a part of a smart sensing system based on FBG sensors and PZT sensors, we have developed an onboard SHM instrument that interrogates the central wavelengths of FBG sensors and impedances of PZT sensors.

Strain distribution on a wing due to flight load is measured by a wavelength interrogator of low sampling rate and recorded continuously. Fast impact signals such as bird strikes necessitate a high sampling rate wavelength interrogator that enables to identify the impact location and estimate the impact-induced damages. Also the impedance spectrum changes of PZT sensors are used to monitor bolt integrity of a fitting lug.

2 Hardware Development

2.1 Low-speed FBG interrogator

FBG wavelength shift is directly proportional to physical strain of the sensing fiber and the central wavelength needs to be interrogated by an opto-

electric hardware. Among the various wavelength interrogation schemes proposed during a couple of decades [1], we have adopted a method based on a broadband light source and a spectrometer because the same platform could be used for high multiplexing or high speed sampling rate.

A super-luminescent diode was used as a broadband light source. Reflected optical signal from FBG sensors is dispersed by a bulk phase grating and imaged on a photodiode array at a focal plane, where a charge-coupled device (CCD) converts photocurrents to voltage signals. The central wavelength among a reflected partial spectrum corresponding to each FBG was found by a Gaussian curve fitting method. In order to accommodate lots of fiber strands, we used a micro-opto-electro-mechanical switch routing several optical fiber lines sequentially. The sampling rate of an off-the-shelf CCD spectrometer is kHz range or so in general because CCD read-out circuitry is usually built with multiplexing technique for hundreds of pixels to be addressed sequentially in time [2].

The spectrometer consisted of 512 photodiodes and covered over 85nm spectral range. So more than 24 FBG sensors per fiber core could be interrogated simultaneously. A field-programmable gate array (FPGA) was used to retrieve reflected spectrum from the FBG sensors and identify each peak from the spectrum. A digital signal processor (DSP) was used to extract the central wavelength of each FBG sensor and to convert it to strain signal and calculate flight load with a neural network algorithm.

We also implemented auto-gain function to adapt varying level of reflected FBG signals by up to 40dB. Because strain measurement should be repeatable against operational environment such as temperature, humidity and atmospheric pressure, we included an automatic wavelength correction algorithm by using

a standard gas absorption cell that was repeatedly measured by the same spectrometer. The upper part of Fig.1 indicates schematic configuration and Fig.2 shows the corresponding printed circuit board of the

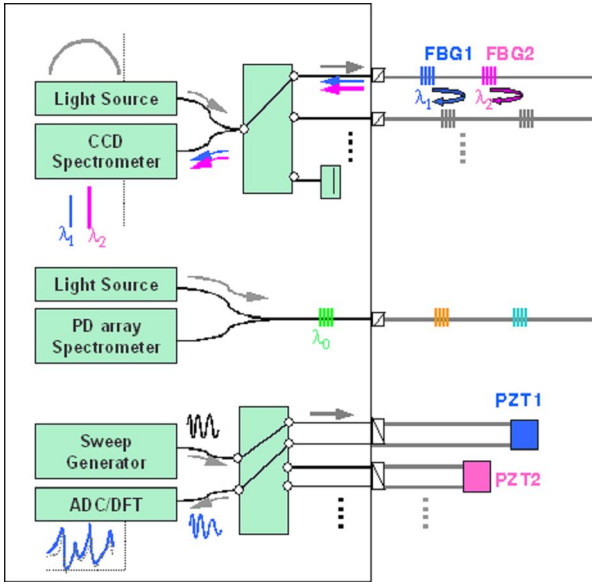


Fig.1. Configuration of an integrated onboard SHM system.



Fig.2. Printed circuit board and assembly for monitoring flight load operating at 200Hz sampling rate.

prototype. The resolution and the uncertainty of the measured strain was less than $0.5\mu\epsilon$ and $10\mu\epsilon$ respectively as shown in Fig.3 that confirmed by a calibrated wavelength meter.

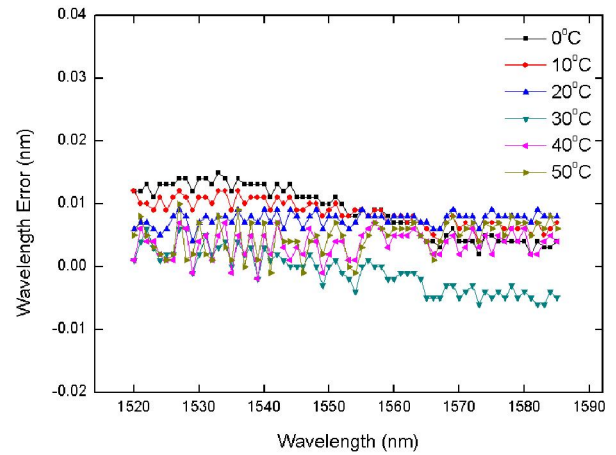


Fig.3. Central wavelength errors over operational wavelength range at various temperatures.

2.2 High-speed FBG interrogator

In order to increase sampling rate of wavelength interrogation, we made all-parallel signal processing from the analog-front end instead of the conventional CCD read-out circuit [3]. Thus each photodiode is followed by its own amplifier and analog-to-digital converter (ADC). We could achieve sampling rate of 100kHz in this way, which was just limited by the sampling rate of the selected ADCs. This approach enabled us to adopt the same optical platform as the previous low-speed type as shown in the middle of Fig.1.

Since the available number of the analog amplifiers and ADCs was practically restrained in terms of the board space, the optical resolution of the spectrometer was increased compared to the low-speed one. We used 80 photodiodes at which a wavelength range of 30nm was dispersed. With the help of the FPGA and the DSP, this board could catch strain signals in real-time triggered by a preset threshold level for impact events. Because strain or temperature information comes from the FBG central wavelength change, the wavelength interrogator has to identify FBG peaks, and take 7 successive pixels imaged by each FBG peak for digital signal processing at first. A Gaussian function that is the closest profile to the FBG reflection spectrum in general, was used as a curve fitting profile.

The least mean-square-error between a Gaussian profile and the measured spectrum was converged within 10 iterations that brought out the central wavelength. However the Gaussian fitting processing was not appropriate for impact signals in real-time because the processing time for a single wavelength interrogation took around $50\mu\text{sec}$ with the floating-point type DSP operating at a 300MHz clock. Instead of using the Gaussian curve fitting processing, we used a centroid calculation that is fast enough, simple to implement into real-time hardware and very robust compared to the non-linear curve fitting processing.

A FBG was glued on a stack type piezo-transducer that was driven by a voltage waveform of 10kHz frequency. The strain response of the FBG was measured by the interrogator and shown in Fig. 4. The noise of the interrogated wavelength was less $0.5\mu\epsilon$ and the amplitude of stain was $7\mu\epsilon$. The red circles correspond to the sampled data and the blue dotted curve is an artificial line that guides the measured data points to the driving waveform.

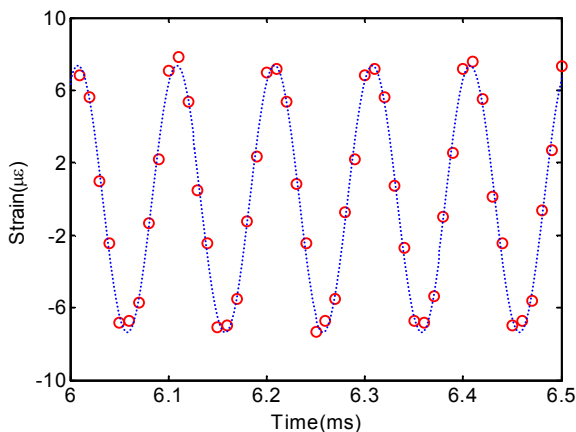


Fig.4. Sinusoidal strain waveform interrogated at sampling rate of 100kHz. The frequency of a driven strain signal is 10kHz and the amplitude is $7\mu\epsilon$.

While the centroid calculation is executed continuously in order to catch any sudden impact events above a given threshold, a sequence of the spectral data is temporally saved on an internal memory too. When an event is met with the threshold condition, the spectral data are retrieved and Gaussian fitting processing is carried out with them. Then finally low-noise strain waveforms are

recorded, and impact location and energy is calculated with the measured strain waveforms.

We could measure propagating impact strain signals simultaneously at 4 FBG sensors glued on the corners of a composite panel. When an applied impact load is not of the center of the panel, the arrival time at a FBG would be different from each other as shown in Fig. 5. From the differences of the arrival time at each FBG sensor, we could estimate the impact location [4]. Impact energy could be estimated too by integrating stain magnitudes over time of the acquired waveforms. Since required level of impact load could be pre-programmed, any impact signal higher than a threshold can be captured automatically and saved in the internal memory of the prototype.

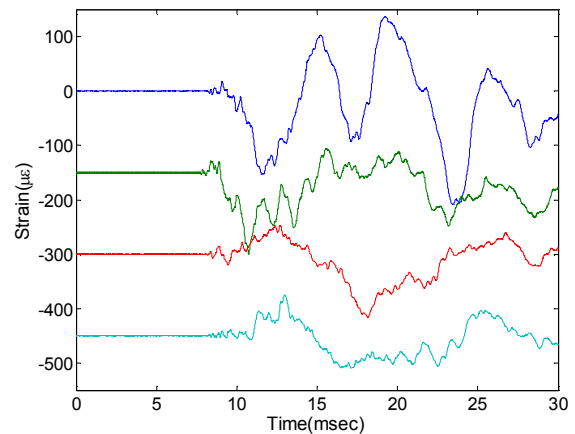


Fig.5. Simultaneously captured strain waveforms on a composite panel when an impact load was applied.

2.3 PZT impedance interrogator

The single electronic integrated chip of AD5933 carries out all the necessary functions regarding impedance measurement. It generates sinusoidal current waveforms with varying frequency to a device under test and converts the induced voltage signals over the PZT sensor to digital values. And it carries out discrete Fourier transform to make impedance spectrum.

We used two sets of AD5933s, multiplexers and amplifiers to drive 12 PZT sensors. The frequency scan range can be set from 1kHz to 100kHz. The impedance level is in the range of $0.1\text{k}\Omega$ to $10\text{k}\Omega$ to comply with those of the PZT sensors glued on the fitting lug. The measured impedance spectrum for a

PZT sensor is compared with that of an impedance analyzer (HP4395A) in Fig 6. The global features are similar to each other except a little difference that was induced by changing of the sensor structure. After measuring impedance spectrum for each sensor, the DSP calculates to extract main features from the spectrum in order to reduce the amount of data to be processed, such as sum, squared sum, root-mean-square, centroid and 1st moment over the impedance spectrum. Next, these features are normalized and projected on the principal components produced from a trained data set using a Gaussian kernel [5]. At last, the DSP calculates the magnitude of the projected features on the principal components and compares it with a threshold value to decide whether it exceeds a threshold value or not. The unit was also used to generate training data set by automatically logging the features because the threshold value can be intentionally lowered to record raw data.

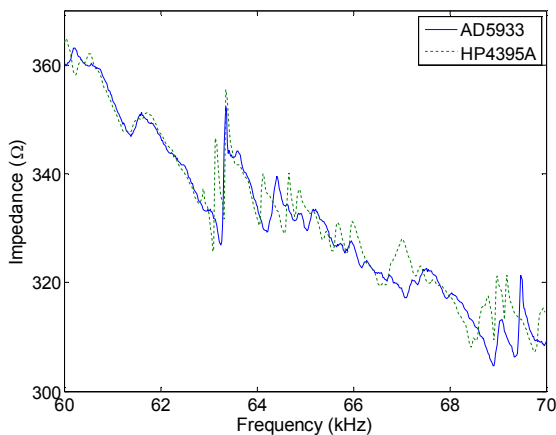


Fig.6. Typical impedance spectrum of a PZT sensor.

3 Performance

Slowly varying strains on a wing structure due to flight load were easy to multiplex more than 100 FBG sensors by using the low-speed wavelength interrogator that could sense 24 sensors on a single fiber. The interrogator recorded the measured strain data on the internal memory as well as calculated flight load and generated an alarm signal in case of overload. For monitoring impact events, the interrogator of 100kHz sampling rate has been developed. The noise and repeatability were about $0.5\mu\epsilon$ and $5\mu\epsilon$ respectively for both of FBG

interrogators. Any impact event above a preset threshold could be captured and recorded successfully. Also impact location and energy could be calculated based on a neural network algorithm. Along with the two FBG interrogators, impedance interrogator was integrated in a single housing of which size was 200 X 140 X 300 mm³ and weighed 4.5kg. The total power consumption was less than 15W and the prototype system performed as a standalone SHM instrument.



Fig.7. Prototype SHM instrument equipped with two FBG interrogators and a PZT impedance interrogator.

References

- [1] A. D. Kersey, M. A. Davis, H. J. Patrick, M. LeBlanc, K. P. Koo, C. G. Askins, M. A. Putnam and E. J. Friebele "Fiber grating sensors". *J. Lightwave Technol.* Vol. 15, pp 1442-1462, 1997.
- [2] G. Li, T. Guo, H. Zhang, H. Gao, J. Zhang, B. Liu, S. Yuan, G. Kai and X. Dong "Fiber grating sensing interrogation based on an InGaAs photodiode linear array". *Appl. Opt.* Vol. 46, pp 283-286, 2007.
- [3] Y. Sano and T. Yoshino "Fast optical wavelength interrogator employing arrayed waveguide grating for distributed fiber Bragg grating sensors". *J. Lightwave Technol.* Vol. 21, pp 132-139, 2003.
- [4] J. A. Greene, T. A. Tran, A. Murphy and R. O. Claus "Optical fiber sensing technique for impact detection and location in composites and metal specimens". *Smart Mater. Struct.* Vol. 4, pp 93-99, 1995.
- [5] C. K. Oh, H. Sohn and I. H. Bae "Statistical novelty detection within the Yeongjong suspension bridge under environmental and operational variations". *Smart Mater. Struct.* Vol. 18, pp 1-9, 2009.